Computer-Aided Design of Novel Siderophores: Pyridinochelin

Michael Meyer[a,*], Rüdiger Schnurre[b], Rolf Reissbrodt[c] and Wolfram Trowitzsch-Kienast[b,*]

[a] Konrad-Zuse-Zentrum für Informationstechnik Berlin, Takustr. 7, D-14195 Berlin, Germany. Fax: +493084185107.
[b] Technische Fachhochschule Berlin, FB II, Luxemburger Str. 10, D-13353 Berlin, Germany. Fax: +493045042011.
[c] Robert-Koch-Institut, D-38855 Wernigerode, Germany

* Authors for correspondence and reprint requests

Z. Naturforsch. **56 c,** 540–546 (2001); received February 13/March 14, 2001

Catecholate-Type Siderophore, Iron Transport, Molecular Modelling

Pyridinochelin, a novel tetradentate catecholate-type siderophore, has been designed on the basis of the active analog enterobactin and was then synthesized. Growth promotion tests indicate that this synthetic siderophore feeds various pathogenic bacteria most effectively with iron even though it lacks one catecholate group compared to enterobactin. The superposition of the mentioned siderophore structures suggests that the structure of the skeleton connecting the catecholate groups might be an important factor for the iron transport.

Introduction

Bacteria produce siderophores, highly specific low molecular weight ligands, for iron supply (Raymond *et al.*, 1984; Raymond, 1994; Neilands, 1995; Drechsel and Jung, 1998; Drechsel and Winkelmann, 1997; Rosenberg *et al.*, 2000). We have designed novel ligands because it is a promising strategy to use conjugates of siderophores and antibiotics as a Trojan horse in order to increase the concentration of the latter only at the site of action (Rosenberg *et al.*, 2000). Furthermore, siderophores can be used to promote the growth of bacteria to facilitate diagnostics. They can be used also in the medical treatment of patients suffering from an excess of iron ions and they are useful for the medication of viral infections. Doerr *et al.* (1995) proved siderophores to interfere with the uridine uptake into the viral DNA. Shanzer and others demonstrated antibiotic activities of siderophores, especially for lipophilic complexing agents, against the *Plasmodium falciparum* causing malaria (Hider and Liu, 1997; Shanzer *et al.*, 1991; Raventos-Suarez *et al.*, 1982; Golenser *et al.*, 1995; Jenett-Siems *et al.*, 1999). Most applications require that a synthetic ligand has a specific structure to be able to form complexes with iron *and* to be recognized by the receptor.

We have designed and synthesized an effective novel iron transporter of the catecholate[2,3-dihydroxy benzoate(DHB)]-type termed Pyridinochelin (bis-2,3-dihydroxybenzoyl-2,6-dimethylamino-pyridine (**1**)) using an active analog approach. Enterobactin (ent,**2**) provides an ideal basis for active analog modeling because the formation constant of $[Fe(ent)]^{3-}$ is about 10^{52} while the affinity towards alkali and alkaline earth metals tends to be much lower. The structures of the $[M(ent)]^{3-}$ anions do not have rotatable bonds eliminating the problem to find out the bioactive conformation from a set of potential conformations for active analog modeling. The enterobactin receptor FepA seems to be an unique bacterial receptor of siderophores recognizing the DHB group in nature. The structure of FepA has been determined recently (Buchanan *et al.*, 1999), but as the electron density in the putative binding region of **2** (Scheme 1) was not well defined, structure based design techniques could not be used. Furthermore, these methods focus on the design of molecules which bind specifically to a protein with a high affinity (Böhm, 1996; Böhm and Klebe, 1996; Marrone *et al.*, 1997; Amzel, 1998; Meyer and Schomburg, 1999), but ligands derived this way might be poor iron transporters. Another complication is the high degree of protein flexibility involved in iron transport, because the FepA is believed to act like an air lock with two hatches in iron transport through the pore.

0939–5075/2001/0700–0540 $ 06.00 D

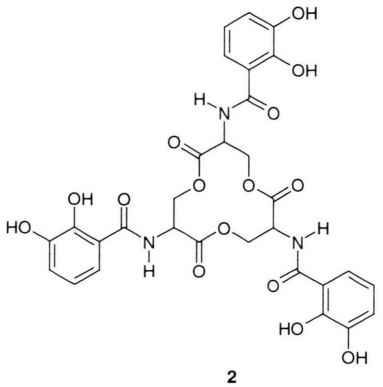

2

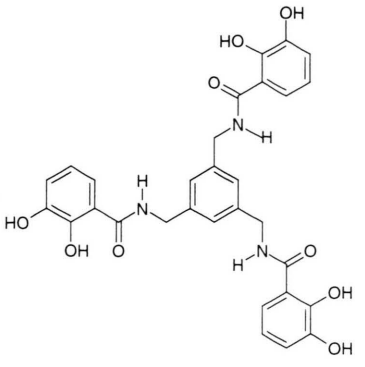

3

Scheme 1. Enterobactin (**2**) and MECAM (**3**) were selected as active analogs for the design of pyridinochelin (**1**) (see Scheme 2).

2 is a natural catecholate-type siderophore with a trilactone ring anchoring skeleton consisting of three L-serine residues, which induce a Δ-configuration of the three bidentate catechol groups at the metal nucleus (right handed propeller). In addition to Fe^{III}, **2** forms isostructural complexes with Ga^{III}, Cr^{III} and V^{IV} (Ised *et al.*, 1976; Raymond *et al.*, 1976; Stack *et al.*, 1992; Karpishin *et al.*, 1993). These ions have been used often in theoretical and experimental studies as a model for iron, because the ionic radii are very similar to that of the ferric ion.

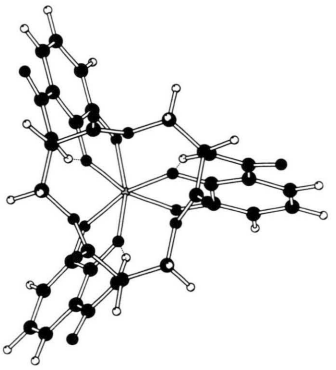

Fig. 1. Calculated $[Ga(ent)]^{3-}$ structure.

Results and Discussion

Computations

The structures of the Ga^{III} complexes with the ligands **2** (Fig. 1) and **3** have been optimized at HF/6–31G(d) level (Hehre *et al.*, 1972; Francl *et al.*, 1982) with Gaussian94 (Frisch *et al.*, 1995) for the Δ-configuration. In order to generate a pseudoreceptor restricting the size of putative ligands, the V^{IV} (Karpishin *et al.*, 1993) and Ga^{III} complexes with **2** and MECAM **3** (Harris and Raymond, 1979), a synthetical siderophore with a nonchiral backbone, have been superimposed using a least squares fit of the metal atoms and all catechol oxygen atoms. Default parameters have been used for both programs, except for a maximal RMS of 0.04 nm in the active analog mode of LUDI (Böhm, 1992; Böhm, 1992a; Böhm, 1996a).

Interaction sites, donor or acceptor sites located at the corresponding atom positions within the receptor, are derived from the complexes. In the next step pharmacophores assumed to be important for metal binding and transport were selected and placed inside the cavity. The selection of the pharmacophore was derived from previous iron uptake investigations with different ligands. These experiments show that the absolute configuration at the iron atom is essential for iron uptake. In contrast to the natural Δ-enterobactin, synthetical Λ-enantio enterobactin (left handed propeller) derived from D-serine does not support growth (Raymond *et al.*, 1984). Consequently the first pharmacophore consists of the tris-catecholamide moiety adopting the Δ-configuration as in natural complexes. We decided to leave the amide group at the catechol rings unchanged, because a previous study with derivatives of MECAM has shown that iron uptake is greatly reduced if the amide groups are alkylated or if the carbonyl and methylene functions are interchanged (Raymond *et al.*, 1984). In the first case intra molecular hydrogen bonds between the amide hydrogen atom and the ortho-oxygen atom (Fig. 1) were made impossible, the

latter case might indicate that the carbonyl groups are involved in hydrogen bonding with FepA. Previous analogs of **2** retained three catecholate groups whereas we prove here that molecules with *bis*-catecholate moieties are efficient iron transporters in bacteria. This hypothesis has been derived from our previous conclusion that certain ligands are able to promote the growth of bacteria (Ambrosi *et al.*, 1998) even though they are only able to use two from three catecholate groups for the binding of a single metal ion (Meyer and Trowitzsch-Kienast, 1997). If less than 6 coordination groups are available, complexes with a ratio between the metal and the ligand different from 1:1 may be formed like in other siderophores (Neilands, 1995) or water molecules may be added to form octahedral complexes.

In the final step a search for suitable fragments was performed in order to link the pharmacophore to a complete molecule with an anchoring skeleton. These fragments had to satisfy three conditions. They must be small enough to fit into the cavity, the atom types of the fragments should correspond to the interaction sites derived from the active molecules and third, the geometry of the fragments has to be suitable to link the pharmacophore without strain. The superposition of the most interesting fragment proposed by LUDI, 2,4-dimethyl thiazole, with the skeleton shows that the nitrogen acceptor atom of this fragment corresponds to the serine side chain oxygen acceptor atom OG. The dimethyl thiazole geometry fits snugly into the skeleton geometry of $[M(ent)]^{3-}$. The distance between both methyl group carbon atoms of 2,4-dimethyl thiazole is 0.4932 nm at HF/6–31G(d) level, whereas the corresponding distance between the methylene carbon atoms is 0.4649 ± 0.0074 nm in the X-ray structure of $[V(ent)]^{3-}$ and 0.4712 nm in the calculated structure of $[Ga(ent)]^{3-}$.

In contrast to the alkyl chain linkers, aromatic rings are more rigid and thus probably freeze the bioactive conformation. Therefore we computed the geometries of further potential heteroaromatic linkers. The distances between both methyl group carbon atoms of 2,6-dimethyl pyridine is 0.4825 nm and therefore this linker is able to fix the catecholamide groups of **1** in a conformation corresponding to the one of complexes with **2**. Apart from the different number of catecholamide groups it is related to **3** (Harris and Raymond, 1979) having a mesitylene fragment in the skeleton. However **3** does not contain any acceptor atom in the skeleton, which probably leads to the less effective iron transport compared to **2**. In contrast, **1** has a single acceptor atom N, which can be superimposed on the serine side chain oxygen atom OG in the lactone ring (Fig. 2). In the siderophore with a 2,4-dimethylthiazole linker even the

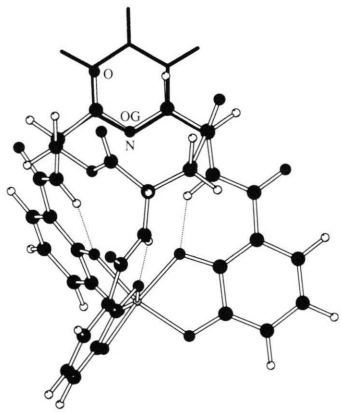

Fig. 2. Superposition of the 2,6-dimethyl pyridine linker (bold) on the skeleton of the calculated $[Ga(ent)]^{3-}$ structure.

carbonyl oxygen atom O is mimicked by the sulfur atom, but it is not known whether the carbonyl oxygen is involved in hydrogen bonds with FepA or not. As **1** shows probably multiple binding sites and ligand orientations at the experimental structure of FepA (Buchanan *et al.*, 1999) and some relevant coordinates are missing in the protein structure, we could not compare the pseudoreceptor with the biopolymer structure. In contrast to **1** selected as a first test of our hypothesis, the phenyl rings of 3,5-bis(*ortho*-hydroxyphenyl)-1,2,4-triazole (Heinz *et al.*, 1999) cannot adopt a conformation like the ones of $[M(ent)]^{3-}$ and acceptor atoms corresponding to the carbonyl oxygen atoms are missing.

Synthesis and physicochemical properties

Since the 2,6-bis-methylamino-pyridine (**4**) was a well known compound produced by the Gabriel synthesis from bis-2,6-bromomethyl-pyridine and phthalimide (Buhleier *et al.*, 1978), the synthesis of **1** was straight forward (Scheme 2). Providing **4** by the described way, we only had to combine the

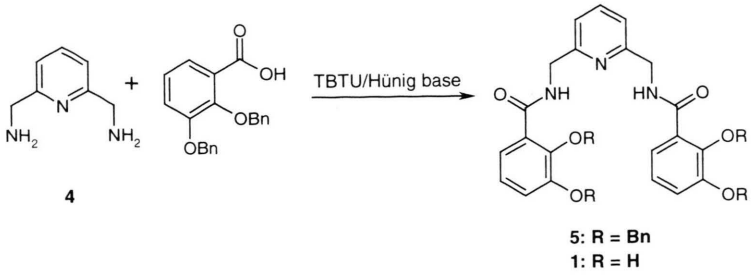

Scheme 2. Synthesis of pyridinochelin (**1**).

diamine-**4** with the benzyl protected 2,3-dihydroxy benzoic acid (Ambrosi *et al.*, 1998) to get the protected di-amide **5**. For this purpose we used the TBTU/Hünig-base approach [TBTU = O-(benzotriazol-1-yl)-N,N,N′,N′-tetramethyluronium tetrafluoroborate]. Deprotection to **1** was achieved smoothly by hydrogenation with the Pd/charcoal catalyst. Because of the availability of the 2,6-bis-hydroxymethyl-pyridine (**6**), we also prepared **4** on an alternative way by transforming **6** into the di-mesylate **7**, and that into the di-azide **8** (Scheme 3). We could isolate **4** in good yields by catalytic reduction on Pd/charcoal.

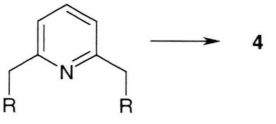

6: R = OH
7: R = OMes
8: R = N_3

Scheme 3. Alternative route from **6** to **4** with the intermediates di-mesylate **7** and di-azide **8**. **4** is used in the synthesis pathway to **1**.

Bis-2,3-dihydroxybenzoyl-2,6-dimethylamino-pyridine (**1**): mp 210 °C; tlc (Kieselgel, Merck SiF_{60}, : 0.60 (DCM+10% MeOH); ^{1}H-NMR (CD_3OD, 600 MHz) δ (ppm) = 7.79 (t, J= 7.75 Hz, 1H, pyridine 4-H), 7.33 (d,*J* = 7.76 Hz, 2H, pyridine 3-H and 5-H), 7.31 (dd, J_1 = 1.36 Hz, J_2 = 7.85 Hz, 2H, 2 × DHB 4-H or 6-H), 6.99 (dd, J_1= 1.35 Hz, J_2= 7.85 Hz, 2H, 2 × DHB 6-H or 4-H), 6.76 (t, *J* = 7.98 Hz, 2H, 2 × DHB-5-H), 4.74 (s, 4H, 2 × -C**H**$_2$-NH-); ^{13}C-NMR (CD_3OD, 300.1 MHz): δ (ppm) = 171.5 (2 × amide-**C**O), 158.7 (pyridine C-2 and C-6), 150.2 and 147.3 (2 × DHB C-2 and C-3), 1329.2 (pyridine C-4), 121.1, 119.8 and 118.9 (2 × DHB C-4, C-5, C-6 and pyridine C-3 and C-5), 116.7 (2 × DHB C-1), 45.4 (2 × -**C**H$_2$-NH); UV λ_{max} (ε) = 315 nm (5.400); FAB-MS (negative mode) *m/z* (%) 408.3 (100)[M-H]$^-$, 272.4 (70)[M-H-DHB]$^-$; FAB-MS (positive mode) *m/z* (%) 432.3 (100) [M+H+Na]$^+$, 410.4 (85)[M+H]$^+$; Anal. ($C_{21}H_{19}N_3O_6$) C calcd., 61.61; found 61.45; H: calcd., 4.68; found, 4.71; N: calcd., 10.26; found, 10.15.

Bis-2,3-dibenzyloxybenzoyl-2,6-dimethylamino-pyridine (**5**): mp 116 °C; ^{1}H-NMR ($CDCl_3$, 400 MHz) δ 8.64 (t, *J* = 5.2 Hz, 2H, 2 × -CH$_2$-N**H**), 7.72 (m, 2H, DHB), 7.50 (t, *J* = 7.73, 1H, Pyridine-4-H), 7.42–7.31 (m, 11 H, arom. H), 7.17–7.06 (m, 15 H, arom. H), 5.09 (s, 4H, 2 × -O-C**H**$_2$-), 4.99 (s, 4H, -O-C**H**$_2$-), 4.46 (d, *J* = 5.2 Hz, 4H, 2 × -C**H**$_2$-NH-); ^{13}C-NMR ($CDCl_3$, 100.6 MHz) δ (ppm) = 165.28 (s, 2 × C=O), 156.69 (s, 2 × =**C**-O-CH$_2$-), 151.91 (s, 2 × =**C**-O-CH$_2$-), 146.90 [s, 2 × -C(=O)-**C**=], 137.26 (d, pyridine-C-4), 136.5 (s, 2 × benzyl-C-1), 136.2 (s, 2 × benzyl-C-1), 128.78, 128.67, 128.43, 128.38, 128.24, 127.71 (all d, 28 × arom. C), 124.40 (d, 2 × arom. C-H), 123.3 (d, 2 × arom. C-H), 120.15 (d, 2 × arom. C-H), 117.07 (d, 2 × arom. C-H), 76.22 (t, 2 × -O-**C**H$_2$-phe), 71.34 (t, 2 × -O-**C**H$_2$-phe), 45.14 (t, 2 × -**C**H$_2$-NH-); EI-MS *m/z* (%) 769 (39), [M]$^+$, 678 (100)[M-benzyl]; Anal. ($C_{49}H_{43}N_3O_6$) C calcd., 76.44; found., 76.52; H: calcd., 5.63; found, 5.66; N: calcd., 5.46; found, 5.31.

Biological studies

To determine the siderophoric activity we carried out growth promotion tests by seeding the iron-starved siderophore-indicator strains listed in Table I into iron-depleted nutrient agar media (Reissbrodt *et al.*, 1993). Each batch of these plates was controlled with natural siderophores. Filter paper discs were loaded with 1 µg of **1** and **2**, as estimated by UV-spectroscopy. Cross-feeding

Table I. The siderophoric capacity[a)] of pyridinochelin (**1**) at diverse pathogenic bacteria with growth zones (GZ).

Species	GZ [mm]
Pseudomonas aeruginosa PAO 6609	16
Yersinia enterocolitica H 5030	24
Aeromonas hydrophila SB 22	*lysis*[a)] 14; 34
Klebsiella pneumophila KN 4401	0
Salmonella thyphimurium TA 2700	44
Salmonella typhimurium WR 1223	45
Salmonella thyphimurium enb-7	44
Salmonella enteritidis P 125109	40
Escherichia coli AB 2847	28
Escherichia coli(tonB)	0
Mycobacterium smegmatis 987	28

[a)] Experimental details are given in the text.
[b)] Lysis means inhibition for higher concentrations of **1**, growth promotion with low concentrations only.

plates with these dried discs on the surface were incubated at least 20 h at of 37 °C (*S. typhimurium*, *Klebsiella pneumophilia*, *E. coli*, *M. smegmatis*) and 30 °C (*P. aeruginosa, Y. enterocoliticia*), respectively. All tests were performed at least twice. Cross-feeding tests yield the growth promotion of **1** relative to **2**.

Tetradentate siderophores like azotochelin and amonabactins have been described previously (Duhme *et al.*, 1998; Telford *et al.*, 1998). But up to now it was an unwritten law that an effective siderophore for iron transport has to have a hexadentate ligand system. Consequently we gave **1** only a little chance to be a good siderophore. But, in contrast, it turns out to be one of the best hitherto known synthetic siderophore, even better than **2**. Table I outlines the extraordinary capacity of **1** as a siderophore determined with growth promotion tests (Reissbrodt *et al.*, 1993). The diameters of the growth zones measured in mm correlate with the siderophoric capacity showing its activity in the nanogram-range comparable with activities measured for **2**. In contrast, Bis 2,3-dihydroxybenzoyl-2-methylamino pyridine lacking one catecholamide group relative to **1** is completely inactive (data not shown).

Some important conclusions can be drawn from the above results. **1** cannot feed *E. coli* bacteria lacking the enterobactin and the tonB system. This proves **1** to use besides the FepA receptor the tonB mediated enterobactin transport system. *Klebsiella pneumophila* was said to possess also the enterobactin transport and utilization system but **1** does not promote the growth of these bacteria. In contrast, **1** very effectively promoted growth of *Mycobacterium smegmatis*. However, **2** is unable to promote this strain (Matzanke *et al.*, 1997), hence the effective uptake of **1** by *M. smegmatis* requires a different uptake system.

Amonabactins, tetradentate ligands, cannot singly satisfy the octahedral coordination sphere of iron. It is the M_2L_3 complex which fully satisfies the coordination geometry of the ferric ion. The behaviour of the 1:1 ferric amonabactin complexes should be comparable to that observed for the dihydroxybenzoylserine linear dimer derived from **2** (Telford *et al.*, 1998). **2** and amonabactin promoted a number of Gram-negative bacteria as *S. thyphimurium*, *E. coli, E. agglomerans, Y. enterocolitica and P. aeruginosa (*Rabsch *et al.*, 1991*)*. Amonabactins promoted the *Salmonella enterica serovars, S. thyphimurium, S. enteritidis, S. agona, S. stanleyville*, but not the host-adapted *Salmonella enterica serovars S. typhi, S. paratyphi A, S. abortusovis, S. pullorum*, whereas **2** promoted growth of all *Salmonella eneterica serovars* mentioned above (Rabsch and Winkelmann, 2000). **1** showed at least the same microbiological activity as enterobactin against different Gram-negative bacteria and also to *M. smegmatis*. Checking the growth promotion of **1** in a cross-feeding test in comparison with freshly isolated **2** produced by the FepA mutant *E. coli* AN 311 (Langman *et al.*, 1972), *S. typhimurium* enb-7 exhibited **1** to be superior since the growth zone was about 50% larger.

Conclusion

We have described a rational strategy for the design of novel siderophores. The derived model suggests that acceptor atoms at the skeleton might be important for efficient iron transport, whereas only two catecholamide groups are required. **1** designed this way acts as a surprisingly active synthetic siderophore for several pathogenic bacteria. The growth zones documented for the *Salmonella* species equal at least the zones generated by **2**. This is the first example for a synthetic tetradentate siderophore with the same activity as **2**. In addition, **1** also feeds mycobacteria quite effectively, one of the objectives for our studies. It should be noted, that **1** exhibits quite good activity against a multi-resistant strain of *Plasmodium falciparum* (Jenett-Siems, 2000).

Acknowledgement

We thank Dr. H. J. Böhm and Dr. S. K. Buchanan for additional information about LUDI and the FepA receptor, respectively. We are grateful to Dr. V. Wray, Mrs. C. Kakoschke and Mr. Christ, all from GBF Braunschweig, who measured the NMR and mass spectra.

Ambrosi H. D., Hartmann V., Pistorius D., Reissbrodt R., and Trowitzsch-Kienast W. (1998), Myxochelines B, C, D, E and F: A new structural principle for powerful siderophores imitated from nature. Eur. J. Org. Chem. 541–551.

Amzel L. M. (1998), Structure-based drug design. Curr. Opin. Biotech. **9**, 366–369.

Böhm H.-J. (1992), The computer program LUDI: A new method for the de novo design of enzyme inhibitors. J. Comput-Aided Mol. Design **6**, 61–78.

Böhm H.-J. (1992a), LUDI: Rule-based automatic design of new substituents for enzyme inhibitor leads. J. Comput-Aided Mol. Design **6**, 593–606.

Böhm H. J. (1996), Computational tools for structure-based ligand design. Prog. Biophys. molec. Biol. **66**, 197–210.

Böhm H.-J. (1996a), Towards the automatic design of synthetically accessible protein ligands: Peptides, amides and peptidomimetics. J. Comput-Aided Mol. Design **10**, 265–272.

Böhm H. J. and Klebe G. (1996), What can we learn from molecular recognition in protein-ligand complexes for the design of new drugs? Angew. Chem. Int. Ed. Engl. **35**, 2588– 2614.

Buchanan S. K., Smith B. S., Venkatramani L., Xia D., Esser L., Palnitkar M., Chakraborty R., van der Helm D., and Deisenhofer J. (1999), Crystal structure of the outer membrane active transporter FepA from *Escherichia coli*. Nature Struct. Biol. **6**, 56–63.

Buhleier E, Wehner W. and Vögtle F.(1978), 2,6-Bis(aminoethyl)pyridin als Komplexligand und neues Kronenethersynthon. Liebigs Ann. Chem., 537–544.

Doerr H. W. Blasko M., Cinatl Jr. J., Hoffmann F., Cinatl J., Weber B., Scholz M., Rabenau H., Stienecker F., and Kabickova H. (1996), *In vitro* inhibiton of human cytomegalovirus replication by calcium trinatrium diethylentriaminepentaacetic acid. Antiviral Research **31**, 23–34.

Drechsel H. and Jung G. (1998), Peptide siderophores. J. Peptide Sci. **4**, 147–181.

Drechsel H. and Winkelmann, G. (1997), Iron chelation and siderophores. In: Transition Metals in Microbial Metabolism (Winkelmann G., Carrano C. J., eds.). Harwood Academic Publishers, London, pp 1–49.

Duhme A.-K., Hider R. C., Naldrett M. J., and Pau R. N. (1998), The stability of the molybdenum-azotochelin complex and ist effect on siderophore production in *Azetobacter vinelandii*. J. Biol. Inorg. Chem. **3**, 520–526.

Frisch M. J., Trucks G. W., Schlegel H. B., Gill P. M. W., Johnson B. G., Robb M. A., Cheeseman J. R., Keith T. A., Petersson G. A., Montgomery J. A., Raghavachari K., Al-Laham M. A.; Zakrzewski V. G., Ortiz J. V., Foresman J. B., Cioslowski J., Stefanov B. B., Nanayakkara A., Challacombe M., Peng, C. Y., Ayala P. Y., Chen W., Wong M. W., Andres J. L., Replogle E. S., Gomperts R., Martin R. L., Fox D. J., Binkley J. S., Defrees D. J., Baker J., Stewart J. P., Head-Gordon M., Gonzalez C., and Pople J. A. (1995), GAUSSIAN 94, Revision B.3, Gaussian, Inc., Pittsburgh PA.

Golenser J., Tsafack A., Amichai Y., Libman J., Shanzer A., and Cabantchik Z. I. Antimalarial action of hydroxamate based iron chelators and potentiation of ferrioxamine action by reversed siderophores. Antimicrob. Agents Chemother., 61–65.

Francl M. M., Pietro W. J., Hehre W. J., Binkley J. S., Gordon M. S., DeFrees D. J., and Pople J. A. (1982), Self-consistent molecular orbital methods. XXIII. A polarization-type basis set for second-row elements. J. Chem. Phys. **77**, 3654–3665.

Harris W. R. and Raymond K. N. (1979), Ferric ion sequestering agents. 3. J. Am. Chem. Soc. **101**, 6534–6541.

Hehre W. J., Ditchfield R., and Pople J. A. (1972), Self-consistent molecular orbital methods. XII. Further extensions of Gaussian-type basis sets for use in molecular orbital studies of organic molecules. J. Chem. Phys. **56**, 2257–2261.

Heinz U., Hergetschweiler K., Acklin P., Faller B., Lattmann R., and Schnebli H. P. (1999), 4-[3,5-bis(2-hydroxyphenyl)-1,2,4-triazol-1-yl] benzoic acid: A novel efficient and selective iron(III) complexing agent. Angew. Chem. Int. Ed. **38**, 2568–2570.

Hider R. C. and Liu Z. (1997), The treatment of malaria with iron chelators. J. Pharm. Pharmacol. 59–64.

Ised S. S., Kuo G. and Raymond K. N. (1976), Coordination isomers of biological iron transport compounds. V. The preparation and chirality of the chromium(III) enterobactin complex and model tris(catechol)chromium(III) analogues. J. Am. Chem. Soc. **98**, 1763–1767.

Jenett-Siems K., Kraft C., Koehler I., Siems K., Jas G., Ambrosi H., Trowitzsch-Kienast W., Mockenhaupt F. P., Bienzle U., and Eich E. (1999), Myxochelins, iron chelators with antimalarial properties. Symposium on Drugs against Parasitic Diseases, Montpellier, France, 24.-16.5.1999, Abstract Book p. 95.

Jenett-Siems K. (2000), FU Berlin, private communication.

Karpishin T. B., Dewey T. M. and Raymond K. N. (1993), The vanadium(IV) enterobactin complex: Structural, spectroscopic, and electrochemical characterization. J. Am. Chem. Soc. **115**, 1842–1851.

Langman L., Young I. G., Frost G. E. and Gibson F. (1972), Enterochelin system of iron transport in *Escherichia coli*: Mutations affecting ferric-enterochelin esterase. J. Bacteriol. **112**, 1142–1149.

Marrone T. J., Briggs J. M. and McCammon J. (1997). Structure-based drug design: computational advances. Annu. Rev. Pharmacol. Toxicol. **37**, 71–90.

Matzanke B. F., Böhnke R., Möllmann U., Reissbrodt R., Schünemann V. and Trautwein A. X. (1997), Iron uptake and intercellular metal transfer in mycobacteria mediated by xenosiderophores. BioMetals **10**, 193–203.

Meyer M. and Trowitzsch-Kienast W. (1997), Computational study of novel catechol-type siderophore analogs. J. Mol. Struct. (Theochem) **418**, 93–98.

Meyer M. and Schomburg D. (1999), Protein interactions. In: Biotechnology, Vol. **5a** (Rehm, H. J. and Reed G., ed.). Wiley-VCH, Weinheim, pp 88–108.

Neilands J. B. (1995). Siderophores: Structure and function of microbial iron transport Compounds. J. Biol. Chem. **270,** 26723–26726.

Rabsch W. and Winkelmann G. (1991) The specificity of bacterial siderophore receptors probed by bioassays. BioMetals **4**, 244–250.

Rabsch W. and Voigt W. (2000), Differences in Fe(III) amonabactin uptake between host-adapted *Salmonella* serovars, including *S. typhi* and *S. paratyphi* A, and non host-adapted *Salmonella* serovars, including *S. enteritidis* and *S. typhimurium*. 2nd International Symposium about Iron Transport, Metabolism and Storage (BioIron 2000), Tübingen, Germany.

Raventos-Suarez C., Pollack S. and Nagel R. L (1982), *Plasmodium falciparum*: Inhibition of in vitro growth by desferrioxamine. Am. J. Trop. Med. Hyg. **31**, 919–922.

Raymond K. N., Ised S. S., Brown L. D., Fronczek F. R. and Nibert J. H. (1976), Coordination isomers of biological iron transport compounds. VI. Models of enterobactin coordination site. A crystal field effect in the structure of potassium tris(catecholato)-chromate(III) and -ferrate(III) sesquihydrates, $K_3[M(O_2C_6H_4)_3]\cdot 1.5\ H_2O$, M=Cr, Fe. J. Am. Chem. Soc. **98**, 1767–1774.

Raymond K. N., Müller G. and Matzanke B. F (1984), Complexation of iron by Siderophores. Top. Curr. Chem **123**, 49–102.

Raymond K. N (1994), Recognition and transport of natural and synthetic siderophores by Microbes. Pure Appl. Chem. **66**, 773–781.

Reissbrodt R., Heinisch L., Möllmann U., Rabsch W. and Ulbricht H. (1993), Growth promotion of synthetic catecholate derivatives on Gram-negative bacteria. BioMetals **6**, 155–162.

Rosenberg J. M., Lin Y.-M., Lu Y. and Miller M. J. (2000), Studies and syntheses of siderophores, microbial iron chelators, and analogs as potential drug delivery systems. Curr. Med. Chem. **7**, 159–197.

Shanzer A., Libman J., Lytton S. D. Glickstein H. and Cabantchik Z. I. (1991), Reversed siderophores act as antimalarial agents. Proc. Natl. Acad. Sci. USA **88**, 6585–6589.

Stack T. D. P., Karpishin T. B. and Raymond K. N. (1992), Structural and spectroscopic characterization of chiral ferric tris-catecholamides: Unraveling the design of enterobactin. J. Am. Chem. Soc. **114**, 1512–1514.

Telford J. R. and Raymond K. N. (1998), Coordination chemistry of the amonabactins, bis (catecholate) siderophores from *Aeromonas hydrophila*. Inorg. Chem. **37**, 4578–4583.